Remarks on the FAI Correlation-based Aerosol Model for SALUS Accident Analysis

Churl Yoon* and Huee-Youl Ye
Versatile Reactor Technology Development Division, Korea Atomic Energy Research Institute,
111 Daedeok-daero 989 Beon-gil, Yuseong-gu, Daejeon 34057, Korea
**Corresponding author: cyoon@kaeri.re.kr*

1. Introduction

Korea Atomic Energy Research Institute (KAERI) has been developing a design and analysis technique for a pool-type sodium-cooled fast reactor called SALUS (Small, Advanced, Long-cycled and Ultimate Safe SFR), which would generate 100MWe with a long refueling period more than 20 years. The ISFRA (Integrated SFR Analysis Program for PSA)[1] computer program can be utilized for simulating the response of the SALUS pool design with metal fuel during a severe accident, which was developed for accident analysis of a PGSFR (Prototype Gen-IV Sodium-cooled Fast Reactor)[2] jointly by KAERI and Fauske & Associates, LLC (FAI). The ISFRA computer program adopts the aerosol correlations of Epstein et al. [3, 4, 5] to predict behavior of non-volatile fission product (FP) aerosols inside a primary coolant system and containment under postulated severe accident conditions, tracking the suspended and deposited aerosol masses.

The ISFRA aerosol model, which is based on the aerosol correlations, provides fast and stable calculations and is based on rigorous analysis. The governing equations for simultaneously coagulating and settling (by gravity) aerosols are transformed into non-dimensional equations based on aerosol similitude, where the particle size distribution reaches a log-normal distribution independent of the initial size distribution after a sufficiently long time. Using the experimental data and analytic solutions, two non-dimensional fits are obtained for the aerosol behavior, one for steady-state and one another for decaying aerosols.

In the previous studies by Yoon and Kang [6, 7], the FAI correlation-based aerosol model has been validated against experimental data and its limitation and advantages were identified. As a closing step of this series of researches on the correlation-based aerosol model, the purposes of this study are to characterize the transition behavior between the steady-state and the decaying modes, and to compare the CPU times between the correlation-based model and the sectional numerical method [8, 9].

2. FAI's correlation-based aerosol model

When $n(v, t)$ is the particle size distribution function, $n(v, t)\mathrm{d}v$ represents the number concentration of particles in the particle volume range v to $v+\mathrm{d}v$ at time t. The equation governing $n(v, t)$ for an aerosol supplied with particles at the constant rate $\dot{n}_p(v)$ and losing mass by deposition on surrounding surfaces at a velocity $u(v)$ is as follows [3]:

$$\frac{\partial n(v,t)}{\partial t} = \frac{1}{2}\int_0^v K(\bar{v}, v-\bar{v}) n(\bar{v},t) n(v-\bar{v},t)\, d\bar{v} - \int_0^\infty K(\bar{v}, v) n(\bar{v},t) n(v,t)\, d\bar{v} - \frac{n(v,t)u(v)}{h} + \dot{n}_p(v) \quad (1)$$

Taking the first moment of Eq. (1) to temporarily avoid the many complications, total suspended aerosol mass concentration $m(t)$ is introduced as below.

$$m(t) = \rho\int_0^\infty v n(v,t)\, dv \quad (2)$$

Eq. (1) becomes the ordinary differential equation for the density of the suspended mass, m.

$$\frac{dm(t)}{dt} = -\lambda(t) m(t) + \dot{m}_p \quad (3)$$

Here, the constant mass rate of production of aerosol particles per unit volume, $\dot{m}_p$, is

$$\dot{m}_p(t) = \rho\int_0^\infty v \dot{n}_p(v,t)\, dv \quad (4)$$

And, λ is the aerosol removal rate constant defined as

$$\lambda(t) = \frac{\int_0^\infty v n(v,t) u(v)\, dv}{h\int_0^\infty v n(v,t)\, dv} \quad (5)$$

To avoid the complexity of the above governing equations, Epstein et al. [3] transformed the aerosol equations to dimensionless forms that readily reveal the nature of the similarities that exist among seemingly different aerosols. The non-dimensional form of major variables derived for aging (decaying) and steady-state aerosols undergoing Brownian and gravitational coagulation and settling are summarized in Table I.

Table I: Non-dimensional form of major variables for aerosols undergoing Brownian and gravitational coagulation and settling

Time, τ	Particle volume, ν	Particle number density, N
$\left(\frac{\alpha g \rho K_0}{\chi^2 \gamma \mu h^2}\right)^{1/2} \cdot t$	$\left(\frac{\gamma g \rho}{\alpha^{1/3} \mu K_0}\right)^{\frac{3}{4}} \cdot v$	$\left(\frac{\gamma^3 K_0{}^5 \mu^5 h^4}{\alpha g^5 \rho^5}\right)^{1/4} \cdot n$
Mass density, M	Decay constant, Λ	Particle production rate, $\dot{N}_p$
$\left(\frac{\gamma^9 g h^4}{\alpha^3 K_0 \mu \rho^3}\right)^{\frac{1}{4}} \cdot m$	$\left(\frac{\gamma \chi^2 \mu h^2}{\alpha K_0 g \rho}\right)^{1/2} \cdot \lambda$	$\left(\frac{\gamma^5 \chi^4 K_0{}^3 \mu^7 h^8}{\alpha^3 g^7 \rho^7}\right)^{\frac{1}{4}} \cdot \dot{n}_p$

To determine the functional relationships $\Lambda(M)$, FAI obtained empirical fitting equations based on many numerical solutions and experimental data. The numerical solutions were obtained by running a sectional analysis tool, the MAEROS code, which was developed by Gelbard et al. [8, 9]. Figure 1 shows the dimensionless removal rate constant as a function of dimensionless suspended aerosol mass concentration, from the measured aerosol mass concentrations of the ABCOVE experiments and several numerical experiments using the MAEROS code. This figure is a reproduction of the similar concept of Figure 1 in Epstein et al. [10].

From the calculated and measured data in Fig. 1, two fitting curves were obtained by FAI. The lower dashed curve corresponds to aerosols continually supplied with particles, under steady-state conditions, in which the loss of particle mass by gravitational sedimentation is balanced by the constant rate of input of particle mass. The upper solid curve is the dimensionless removal rate versus dimensionless mass concentration relation for decaying aerosols in the absence of a source. The obtained algebraic fit equations for the curves are

$$\Lambda_{SED}^{SS} = 0.266M^{0.282}\left(1+0.189M^{0.8}\right)^{0.695} \quad (6)$$

$$\Lambda_{SED}^{D} = 0.528M^{0.235}\left(1+0.473M^{0.754}\right)^{0.786} \quad (7)$$

Here, superscript *SS* indicates when the removal rate constant refers to steady-state conditions, superscript *D* denotes the case of a decaying aerosol, and subscript *SED* denotes particle removal by sedimentation.

SYMBOL	h [m]	$\dot{m}_p$ [kg/m³/s]	ρ [kg/m³]	γ	χ	σ	r_0 [μm]
□	3.1017	9.1549E-7	2450	2.25	1.5	2.0	0.125
△	10.0	8.2160E-6	4000	2.5	1.0	1.55	0.136
○	3.1017	5.9038E-6	2130	2.25	1.5	2.0	0.25
◇	5.0	2.3122E-4	5000	1.0	1.0	1.55	0.27
▽	3.1017	1.1737E-4	3670	2.25	1.5	2.0	0.5
X	2.0	2.9343E-5	2000	1.0	1.0	2.5	1.0
○	1.0	1.1737E-4	1000	1.0	1.0	1.5	0.5

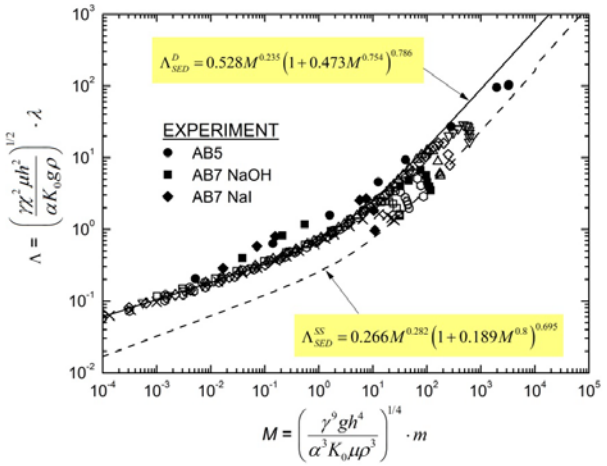

Fig. 1. Dimensionless aerosol removal rate constant for sedimentation as a function of dimensionless suspended mass concentration. (Regeneration of Fig. 1 in Epstein et al. [10])

3. Remarks on the correlation-based aerosol model

3.1 Transition from steady-state to decaying condition

In ISFRA code, the execution procedure to calculate the suspended aerosol masses is as the below:

1) dimensionless suspended aerosol mass M is calculated from the suspended aerosol mass m by using the equations of Table I,
2) dimensionless decay constant Λ is calculated from the value M by using Eq. (6) or (7) depending on the situation of steady-state or decaying aerosol,
3) the dimensionless decay constant Λ is transformed into an aerosol removal rate constant λ by utilizing the equations of Table I, and
4) suspended aerosol mass m is finally calculated by the following equations.

$$\frac{dm(t)}{dt} = -\lambda_{SED}^{SS} m(t) + \dot{m}_p \quad (8)$$

$$\frac{dm(t)}{dt} = -\lambda_{SED}^{D} m(t) \quad (9)$$

To understand the characteristics of the transition behavior between the steady-state and the decaying modes, the airborne aerosol mass m and the aerosol removal rate constant λ_{SED} were tracked more closely for the ISFRA simulation of the ABCOVE AB5 experiments [11]. The predicted airborne aerosol mass of AB5 is shown as a function of time in Fig. 2(a).

In Fig. 2(b), the dimensionless removal rate constant Λ_{SED} is presented as a function of dimensionless suspended aerosol mass density. Note that the airborne aerosol mass m and the aerosol removal rate constant λ_{SED} are converted into dimensionless parameters for easy comparison with Fig. 1. While there is an aerosol source from 0 to 872 s, the aerosol removal rate constant follows the steady-state curve of aerosol removal rate constant. After 872 s when the aerosol source becomes zero, Λ_{SED} now follows the decaying curve of aerosol removal rate constant. During the aerosol source period from 0 to 872 s, the removal rate constant is a small value at the early time due to low aerosol concentration and the Λ_{SED} value increases due to the increasing airborne aerosol concentration as time goes on. During the no-source period after 872 s, the Λ_{SED} value decreases due to the decreasing airborne aerosol concentration as time goes on.

To switch from one of the decaying or the steady-state correlation to another, the FAI correlation-based aerosol model uses an interpolation factor (*FSEDDK*) between decaying and steady-state correlations. To explain this interpolation factor, the steady-state airborne aerosol mass M_{SS} should be calculated first from Eq. (10).

$$\frac{dm(t)}{dt} = -\lambda_{SED} m(t) + \dot{m}_p \quad (10)$$

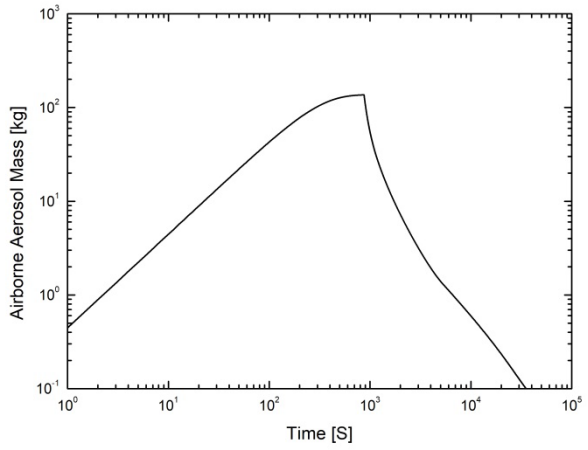

(a) Time .vs. Airborne Aerosol Mass

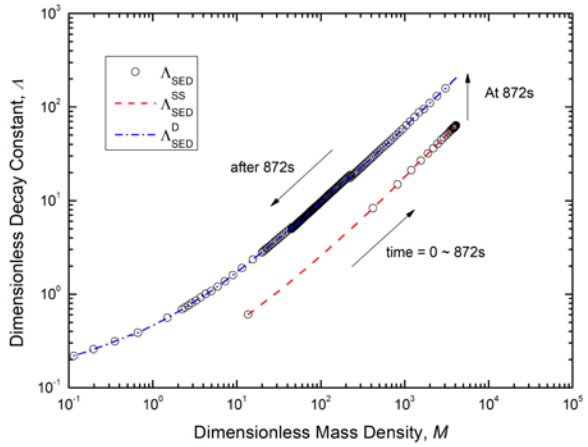

(b) Dimensionless Mass Density .vs. Dimensionless Decay Constant

Fig. 2. Detailed trend of aerosol removal rate constant Λ_{SED} for AB5 prediction.

The time derivative term should be zero when it is steady-state. Then the steady-state airborne aerosol mass M_{SS} becomes

$$M_{SS} = \frac{\dot{m}_p}{\lambda_{SED}} \quad . \tag{11}$$

For each case of the follows, the aerosol removal rate constant λ_{SED} is determined differently.

i) When there is no aerosol source;
$\lambda_{SED} = \lambda_{SED}^{D}$

ii) When there are aerosol sources;
(ii-1) If m(t)/M_{SS} < 1.0, $\lambda_{SED} = \lambda_{SED}^{SS}$.
(ii-2) If m(t)/M_{SS} > 1.0, then

$$U = \frac{m(t) - M_{SS}}{(f_{SS} - 1)M_{SS}}$$. (constant f_{SS} = 8.0 in ISFRA)

Here, f_{SS} is a multiplier to the expected steady-state mass, above which the new source will not affect the removal rate. (> 1.0)

The interpolation factor *FSEDDK* is shown in Fig. 3 as a function of (m(t)/M_{SS}) with a f_{SS} value of 8.0.

$$FSEDDK = 4*U^3 - 6*U^2 + 3*U \tag{12}$$

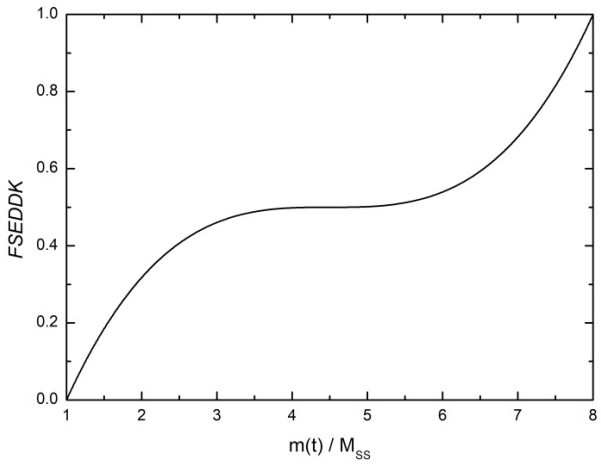

Fig. 3. Trend of the *FSEDDK* variable as a function of the ratio of suspended aerosol mass $m(t)$ to the steady-state airborne aerosol mass M_{SS} (with f_{SS} = 8.0)

Finally, the aerosol removal rate constant λ_{SED} is calculated by the interpolation between λ_{SED}^{SS} and λ_{SED}^{SS}.

$$\lambda_{SED} = FSEDDK * \lambda_{SED}^{D} + (1 - FSEDDK) * \lambda_{SED}^{SS} \tag{13}$$

In the AB5 prediction, the interpolation factor was maintained to be zero from the beginning to 872 s and became one when the aerosol source was removed at 872 s. For this AB5 simulation, since the time duration when $m(t)$ becomes larger than M_{SS} before the removal of the aerosol source is not long enough, the aerosol removal rate constant value immediately jumped from the steady-state to the decaying curve at 872 s. However, if the aerosol source were removed at a later time (> 872 s), the transition from the steady-state correlation to the decaying correlation would occur more smoothly following the curve shown in Fig. 3.

3.2 CPU time comparison

The subroutines related only to aerosol FP analysis were extracted from the ISFRA code and a driver was created to impose the appropriate boundary condition of the experiment. This stand-alone aerosol module of ISFRA was utilized for the CPU time comparison between the MAEROS sectional method and the correlation-based log-normal aerosol model. Since this ISFRA aerosol module does not have the capability to analyze the multi-component aerosol behavior, CPU time comparison was performed only for the AB5 simulation.

Table II shows the resultant values of the CPU time comparison. For the CPU time comparison of basic logics only, the unnecessary procedures were removed and the simulation times were set to be the same value of 300,000 s. Both computations of the sectional and the correlation-based models were performed on the same PC with the 64-bit WINDOWS operating system on an

Table II: CPU time comparison between the sectional and the correlation-based aerosol models, for the ABCOVE AB5 simulation

	Stand-alone aerosol module of ISFRA code	MAEROS sectional model
Simulation condition	time_end = 3.0E+05 sec	28 particle size sections time_end = 3.0E+05 sec
CPU time	0.6250E-01 sec	0.5000E+01 sec

Intel I7-7700 CPU. From this comparison result, it is concluded that the correlation-based aerosol model gives output about 80 times faster than the sectional method in the AB5 simulation.

4. Conclusions

In this final stage of the research series on the FAI correlation-based aerosol model, the transition behavior between the steady-state and the decaying modes was investigated. For the AB5 simulation results, the aerosol removal rate constants as a function of time were extracted and the transition behavior from steady-state to decaying mode was tracked. This transition behavior was found to be controlled by the interpolation factor *FSEDDK*, which is the internal variable of ISFRA code.

The CPU times were compared between the computations by the correlation-based model and by the sectional numerical method. As a conclusion, it was revealed that the correlation-based aerosol model gave output about 80 times faster than the sectional method for the single-component aerosol analysis of the AB5 experiment.

ACKNOWLEDGMENTS

This work was supported by the National Research Foundation of Korea (NRF) grant funded by the Korea government (MSIT). (No. 2021M2E2A1037871)

NOMENCLATURE

g	gravity
h	effective height for aerosol deposition [m]
$K(v, \tilde{v})$	kernel representing the frequency of binary collisions between particles of volume v and $\tilde{v}$
K_0	normalized Brownian collision coefficient ($= 4kT/(3\mu)$)
m	total mass concentration of the suspended aerosols [kg/m^3]
$\dot{m}_p$	aerosol mass production rate [kg/m^3/s]
M	dimensionless total suspended aerosol mass
n	particle size distribution function [m^{-3}]
$\dot{n}_p$	source rate of particles [m^{-3}s^{-1}]
$N(\upsilon,\tau)$	dimensionless particle distribution function
v	particle volume [m^3]
t	time [s]
u	particle deposition or removal velocity [m/s]
α	density correction factor [-]
χ	particle settling shape factor [-]
γ	collision shape factor [-]
λ	aerosol removal rate constant [s^{-1}]
Λ	dimensionless decay constant
μ	viscosity of the carrier gas [kg/m/s]
ρ	density of the aerosol material [kg/m^3]
τ	dimensionless time
υ	dimensionless particle volume

REFERENCES

[1] Fauske & Associates, LLC, ISFRA user manual, FAI Report, FAI/16-1089, p. 10, 2016.
[2] J. Yoo, J. Chang, J.-Y. Lim, J.-S. Cheon, T.-H. Lee, S.K. Kim, K.L. Lee, and H.-K. Joo, "Overall System Description and Safety Characteristics of Prototype Gen IV Sodium Cooled Fast Reactor in Korea," Nuclear Engineering and Technology, Vol. 48, pp. 1059–1070, 2016.
[3] M. Epstein, P.G. Ellison, and R.E. Henry, "Correlation of Aerosol Sedimentation," Journal of Colloid & Interface Science, Vol. 113, No. 2, 1986.
[4] M. Epstein and P. G. Ellison, "A Principle of Similarity for Describing Aerosol Particle Size Distribution", Journal of Colloid & Interface Science, Vol. 119, No. 1, pp. 168-173, 1987.
[5] M. Epstein, G. M. Hauser, and R. E. Henry, "Thermophoretic Deposition of Particles in Natural Convection Flow from a Vertical Plate," Journal of Heat Transfer, Vol. 107, pp. 272-276, 1985.
[6] C. Yoon and S. H. Kang, "Review of the Aerosol Mass Tracking Method in the ISFRA Fission Product Transport Module for SFR Accident Analyses," KNS Spring Meeting, Jeju, May 2020.
[7] C. Yoon and S. H. Kang, "Implementation and Validation of the MAEROS Aerosol Model in ISFRA SFR Severe Accident Analysis Program," KNS Autumn Meeting, Changwon, Oct. 2020.
[8] F. Gelbard, Y. Tambour, and J.H. Seinfeld, "Sectional Representations for Simulating Aerosol Dynamics," Journal of Colloid Interface Science, Vol. 76, pp. 541-556, 1980.
[9] F. Gelbard, The MAEROS User Manual, NUREG/CR-1391, SAND80-0822, Sandia National Labs Report, 1982.
[10] M. Epstein and P. G. Ellison, "Correlations of the Rate of Removal of Coagulating and Depositing Aerosols for Application to Nuclear Reactor Safety Problems", Nuclear Engineering and Design, Vol. 107, pp. 327-344, 1988.
[11] R. K. Hilliard, J.D. McCormack, A.K. Postma, "Results and code predictions for ABCOVE aerosol code validation - Test AB5," HEDL-TME 83-16, 1983.